Proceedings of the ASME 2009 Dynamic Systems and Control Conference
DSCC2009
October 12-14, 2009, Hollywood, California, USA

DSCC2009-2687

DESIRED COMPENSATION ADAPTIVE ROBUST CONTOURING CONTROL OF AN INDUSTRIAL BIAXIAL PRECISION GANTRY SUBJECT TO COGGING FORCES *

Chuxiong Hu
The State Key Laboratory of Fluid Power Transmission and Control
Zhejiang University
Hangzhou, 310027, China
Email: fyfox.hu@gmail.com

Bin Yao†
School of Mechanical Engineering
Purdue University
West Lafayette, Indiana, 47907
U.S.A
Email: byao@purdue.edu

Qingfeng Wang
The State Key Laboratory of Fluid Power Transmission and Control
Zhejiang University
Hangzhou, 310027, China
Email: qfwang@zju.edu.cn

ABSTRACT

To obtain a higher level of contouring motion control performance for linear-motor-driven multi-axes mechanical systems subject to significant nonlinear cogging forces, both coordinated control of multi-axes motions and effective compensation of cogging forces are necessary. In addition, the effect of unavoidable velocity measurement noises needs to be carefully examined and sufficiently attenuated. To solve these problems simultaneously, in this paper, a discontinuous projection based desired compensation adaptive robust contouring controller is developed by explicitly taking into account the specific characteristics of cogging forces in the controller designs and employing the task coordinate formulation for coordinated motion controls. Specifically, based on the largely periodic nature of cogging forces with respect to position, design models consisting of known sinusoidal functions of positions corresponding to the main harmonics of the force ripple waveforms with unknown weights are used to approximate the unknown cogging forces. Theoretically, the resulting controller achieves a guaranteed transient performance and final contouring accuracy in the presence of both parametric uncertainties and uncertain nonlinearities. In addition, the controller also achieves asymptotic output tracking when there are parametric uncertainties only. Comparative experimental results obtained on a high-speed industrial biaxial precision gantry driven by linear motors are presented to verify the excellent contouring performance of the proposed control scheme and the effectiveness of the cogging force compensations.

*THE WORK IS SUPPORTED IN PART BY THE US NATIONAL SCIENCE FOUNDATION (GRANT NO. CMS-0600516) AND IN PART BY THE NATIONAL NATURAL SCIENCE FOUNDATION OF CHINA (NSFC) UNDER THE JOINT RESEARCH FUND FOR OVERSEAS CHINESE YOUNG SCHOLARS (GRANT NO. 50528505).

†Address all correspondence to this author.

1 Introduction

For an industrial biaxial gantry system driven by linear motors, the contouring performance is evaluated by the contouring error which represents the geometric deviation from the actual contour to the desired contour [1]. The degradation of contouring performance could be mainly due to lacking coordination of multi-axes motions [2] and effects of disturbances such as friction and cogging forces [3]. The former is referred to as the coordinated contouring control problem and the later as the disturbance rejection/compensation.

To address the contouring control problems, Koren [4] first proposed the cross-coupled control (CCC) strategy in which coupling actions was introduced in the servo controllers so that the control of one axial servomechanism was affected by other axial servomechanisms involved in the motion and consequently the coordination of axes was strengthened. Since then, many research publications on CCC have been published [2, 5, 6]. But these designs are based on the traditional control theories for linear time-invariant systems and cannot address the dynamic coupling phenomena (e.g. Coriolis force) well when tracking curved contours. Chiu and Tomizuka [7] formulated the contouring control problem in a task coordinate frame "attached" to the desired contour. Under the task coordinate formulation, a control law could be designed to assign different dynamics to the normal and tangential directions relative to the desired contour. Since then contouring control schemes based on task coordinate approaches have been reported [1,8]. However, these control techniques cannot explicitly deal with parametric uncertainties and uncertain

nonlinearities. As a result, they are often insufficient when stringent contouring performance is of concern as actual systems are always subjected to certain model uncertainties and disturbances.

To achieve higher precision motion control of linear-motor-driven systems, the cogging force behavior should be clearly understood such that effective cogging force compensation can be synthesized. Thus significant research efforts have been devoted to the modeling and compensation of cogging force [3, 9, 10]. For example, in [10], the cogging force is assumed to be periodic functions with respect to position so that Fourier expansion with a few significant terms could be utilized to represent the cogging force. Non-periodic effect is also considered in a recent publication [3]. It should be noted all these cogging force compensation researches are done for single axis motion only.

In this paper, high-performance contouring motion control of a biaxial linear-motor-driven precision gantry subject to significant nonlinear cogging forces is studied. In order to achieve effective cogging force compensations, the cogging force model in [10] is utilized to formulate the overall system dynamics in a task coordinate frame. The desired compensation adaptive robust control (DCARC) strategy [11] is then applied to develop a coordinated ARC contouring controller in which the regressor is calculated based on the desired contour information only. Theoretically, the proposed controller achieves certain guaranteed output contouring transient performances and steady-state contouring accuracies even in the presence both parametric uncertainties and uncertain nonlinearities. In addition, when the actual system is subjected to parametric uncertainties only, a much improved steady-state tracking performance – asymptotic output tracking – is achieved as well. Experimental results have also been obtained on a high-speed Anorad industrial biaxial gantry driven by LC-50-200 linear motors with a linear encoder resolution of 0.5 μm. The results verify the excellent contouring performance of the proposed DCARC controller in actual implementation in spite of various parametric uncertainties and uncertain disturbances. Comparative experimental results also demonstrate the effectiveness of the cogging force compensations.

2 Problem Formulation

2.1 Task Coordinate Frame

Figure 1 shows a popular approximation of contouring error [5, 8]. Let x and y denote the horizontal and the vertical axes of a biaxial gantry system. At any time instant, there are two points P_d and P_a denoting the position of the reference command and the actual position of the system, respectively. Tangential and normal directions of the desired contour at the point P_d are used to approximate the contouring error by the distance from P_a to the tangential line. With this definition, the contouring error ε_c can be approximately computed by the normal error ε_n as:

$$\varepsilon_c \approx \varepsilon_n = -sin\alpha \cdot e_x + cos\alpha \cdot e_y \tag{1}$$

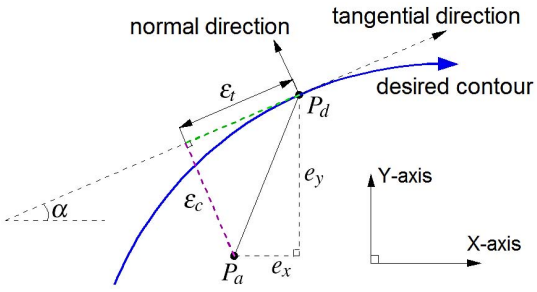

Figure 1. An Approximate Contouring Error Model

where e_x and e_y denote the axial tracking errors of x and y axes, i.e. $e_x = x - x_d$, $e_y = y - y_d$, and α denotes the angle between the tangential line to the horizontal X-axis. In this model, if the axial tracking errors are comparatively small to the curvature of the desired contour, then it yields a good approximation of the contouring error. The tangential error ε_t in Figure 1 can be obtained as

$$\varepsilon_t = cos\alpha \cdot e_x + sin\alpha \cdot e_y \tag{2}$$

Then the tangential and the normal directions are mutually orthogonal and hence can be taken as the basis for the task coordinate frame. Thus the physical (x, y) coordinates can be transformed into the task coordinates of $(\varepsilon_c, \varepsilon_t)$ by a linear transformation

$$\boldsymbol{\varepsilon} = \mathbf{Te} \tag{3}$$

where $\boldsymbol{\varepsilon} = [\varepsilon_c, \varepsilon_t]^T$; $\mathbf{e} = [e_x, e_y]^T$, and the time-varying transformation matrix depends on the reference trajectories of the desired contour only and is given by

$$\mathbf{T} = \begin{bmatrix} -sin\alpha & cos\alpha \\ cos\alpha & sin\alpha \end{bmatrix} \tag{4}$$

The matrix $\mathbf{T}$ is always unitary for all values of α, i.e., $\mathbf{T^T} = \mathbf{T}$ and $\mathbf{T^{-1}} = \mathbf{T}$.

2.2 System Dynamics

The biaxial linear-motor-driven gantry has the following dynamics [3]:

$$\mathbf{M\ddot{q}} + \mathbf{B\dot{q}} + \mathbf{F_c}(\dot{\mathbf{q}}) + \mathbf{F_r}(\mathbf{q}) = \mathbf{u} + \mathbf{d}; \tag{5}$$

where $\mathbf{q} = [x(t), y(t)]^T$, $\dot{\mathbf{q}} = [\dot{x}(t), \dot{y}(t)]^T$ and $\ddot{\mathbf{q}} = [\ddot{x}(t), \ddot{y}(t)]^T$ are the 2×1 vectors of the axis position, velocity and acceleration, respectively; $\mathbf{M} = diag[M_1, M_2]$ and $\mathbf{B} = diag[B_1, B_2]$ are the

2×2 diagonal inertia and viscous friction coefficient matrices, respectively. $\mathbf{F_c}(\dot{\mathbf{q}})$ is the 2×1 vector of Coulomb friction which is modeled by $\mathbf{F_c}(\dot{\mathbf{q}}) = \mathbf{A_f S_f}(\dot{\mathbf{q}})$, where $\mathbf{A_f} = diag[A_{f1}, A_{f2}]$ is the 2×2 unknown diagonal Coulomb friction coefficient matrix, and $\mathbf{S_f}(\dot{\mathbf{q}})$ is a known vector-valued smooth function used to approximate the traditional discontinuous sign function $sgn(\dot{\mathbf{q}})$ used in the traditional Coulomb friction modeling for effective friction compensation in implementation [14]. $\mathbf{F_r}(\mathbf{q})$ represents the 2×1 vector of position dependent cogging forces. $\mathbf{u}$ is the 2×1 vector of control input, and $\mathbf{d}$ is the 2×1 vector of unknown nonlinear functions due to external disturbances or modeling errors.

In this paper, it is assumed that the permanent magnets of the same linear motor are all identical and are equally spaced at a pitch of P. Thus, $\mathbf{F_r}(\mathbf{q}) = [F_r(x), F_r(y)]^T$ is a periodic function of position $\mathbf{q}$ with a period of P, i.e., $F_r(x+P) = F_r(x)$, $F_r(y+P) = F_r(y)$ and it can be approximated quite accurately by the first several harmonic functions of the positions, which is represented by

$$\begin{array}{l} \bar{F}_r(x) = \sum_{i=1}^{m} (S_{xi} sin(\frac{2i\pi}{P}x) + C_{xi} cos(\frac{2i\pi}{P}x)) \\ \bar{F}_r(y) = \sum_{j=1}^{n} (S_{yj} sin(\frac{2j\pi}{P}y) + C_{yj} cos(\frac{2j\pi}{P}y)) \end{array} \tag{6}$$

where $S_{xi}, C_{xi}, S_{yj}, C_{yj}$ are the unknown weights, m and n are the numbers of harmonics used to approximate the cogging forces in X-axis and Y-axis, respectively. The larger m and n are, the better $\bar{\mathbf{F}}_\mathbf{r}(\mathbf{q})$ approximates the actual cogging forces, but the larger the number of parameters need to be adapted. So a trade-off has to be made based on the particular structure of a motor. For example, in [12], it was experimentally observed that the first, the third, and the fifth harmonics are the main harmonics in the force ripple waveform.

With the above cogging force and friction modelling, the linear motor dynamics (5) can be written as:

$$\mathbf{M}\ddot{\mathbf{q}} + \mathbf{B}\dot{\mathbf{q}} + \mathbf{A_f S_f}(\dot{\mathbf{q}}) + \bar{\mathbf{F}}_\mathbf{r}(\mathbf{q}) = \mathbf{u} + \mathbf{d_N} + \widetilde{\mathbf{d}} \tag{7}$$

where $\mathbf{d_N} = [d_{N1}, d_{N2}]^T$ is the nominal value of the lumped modeling error and disturbance $\mathbf{d}_l = \mathbf{d} + \bar{\mathbf{F}}_\mathbf{r}(\mathbf{q}) - \mathbf{F_r}(\mathbf{q}) + \mathbf{A_f S_f}(\dot{\mathbf{q}}) - \mathbf{F_c}(\dot{\mathbf{q}})$, and $\widetilde{\mathbf{d}} = \mathbf{d}_l - \mathbf{d_N}$ represents the time-varying portion of the lumped uncertainties. For this dynamic system, we define the tracking error as $\mathbf{e} = [e_x, e_y]^T = [x(t) - x_d(t), y(t) - y_d(t)]^T$ where $\mathbf{q_d}(t) = [x_d(t), y_d(t)]$ is the reference trajectory describing the desired contour. Then the system dynamics can be rewritten as

$$\mathbf{M}\ddot{\mathbf{e}} + \mathbf{B}\dot{\mathbf{e}} + \mathbf{A_f S_f}(\dot{\mathbf{q}}) + \bar{\mathbf{F}}_\mathbf{r}(\mathbf{q}) + \mathbf{M}\ddot{\mathbf{q}}_\mathbf{d} + \mathbf{B}\dot{\mathbf{q}}_\mathbf{d} = \mathbf{u} + \mathbf{d_N} + \widetilde{\mathbf{d}} \tag{8}$$

Noting (3) and (4) and the unitary property of $\mathbf{T}$, the time derivatives of the tracking error states can be derived as [8]

$$\dot{\mathbf{e}} = \mathbf{T}\dot{\varepsilon} + \dot{\mathbf{T}}\varepsilon, \quad \ddot{\mathbf{e}} = \mathbf{T}\ddot{\varepsilon} + 2\dot{\mathbf{T}}\dot{\varepsilon} + \ddot{\mathbf{T}}\varepsilon \tag{9}$$

Then the system dynamics can be represented in the task coordinate frame as

$$\begin{array}{c} \mathbf{M_t}\ddot{\varepsilon} + \mathbf{B_t}\dot{\varepsilon} + 2\mathbf{C_t}\dot{\varepsilon} + \mathbf{D_t}\varepsilon + \mathbf{M_q}\ddot{\mathbf{q}}_\mathbf{d} + \mathbf{B_q}\dot{\mathbf{q}}_\mathbf{d} \\ + \mathbf{A_{fq}}\mathbf{S_f}(\dot{\mathbf{q}}) + \mathbf{F_{rq}}(\mathbf{q}) = \mathbf{u_t} + \mathbf{d_t} + \widetilde{\Delta} \end{array} \tag{10}$$

where

$$\begin{array}{l} \mathbf{M_t} = \mathbf{TMT}, \mathbf{B_t} = \mathbf{TBT}, \mathbf{C_t} = \mathbf{TM}\dot{\mathbf{T}}, \\ \mathbf{D_t} = \mathbf{TM}\ddot{\mathbf{T}} + \mathbf{TB}\dot{\mathbf{T}}, \mathbf{u_t} = \mathbf{Tu}, \mathbf{d_t} = \mathbf{Td_N}, \widetilde{\Delta} = \mathbf{T}\widetilde{\mathbf{d}}, \\ \mathbf{M_q} = \mathbf{TM}, \mathbf{B_q} = \mathbf{TB}, \mathbf{A_{fq}} = \mathbf{TA_f}, \mathbf{F_{rq}}(\mathbf{q}) = \mathbf{T}\bar{\mathbf{F}}_\mathbf{r}(\mathbf{q}) \end{array} \tag{11}$$

It is well known that equation (10) has the following properties:

(P1) $\mathbf{M_t}$ is a symmetric positive definite (s.p.d.) matrix with

$$\mu_1 \mathbf{I} \leq \mathbf{M_t} \leq \mu_2 \mathbf{I} \tag{12}$$

where μ_1 and μ_2 are two positive scalars.

(P2) The matrix $\mathbf{N}_t = \dot{\mathbf{M}}_\mathbf{t} - 2\mathbf{C_t}$ is a skew-symmetric matrix.

(P3) All modeled terms of the task space dynamics (10) can be linearly parameterized by a set of parameters as follows

$$\begin{array}{c} \mathbf{M_t}\ddot{\varepsilon} + \mathbf{B_t}\dot{\varepsilon} + \mathbf{2C_t}\dot{\varepsilon} + \mathbf{D_t}\varepsilon + \mathbf{M_q}\ddot{\mathbf{q}}_\mathbf{d} + \mathbf{B_q}\dot{\mathbf{q}}_\mathbf{d} \\ + \mathbf{A_{fq}}\mathbf{S_f}(\dot{\mathbf{q}}) + \mathbf{F_{rq}}(\mathbf{q}) - \mathbf{d_t} = -\varphi(\mathbf{q}, \dot{\mathbf{q}}, \ddot{\mathbf{q}}, t)\theta \end{array} \tag{13}$$

where φ is a $2 \times (8 + 2m + 2n)$ matrix of known functions, commonly referred to as the **regressor**, and θ is a vector of unknown parameters defined as $\theta = [\theta_1, ..., \theta_{8+2m+2n}]^T = [M_1, M_2, B_1, B_2, A_{f1}, A_{f2}, S_{x1}, C_{x1}, ..., S_{xm}, C_{xm}, S_{y1}, C_{y1}, ..., S_{yn}, C_{yn}, d_{N1}, d_{N2}]^T$.

In general, the parameter vector θ cannot be known exactly. For example, the payload of the biaxial gantry depends on tasks. However, the extent of parametric uncertainties can be predicted. Therefore, the following practical assumption is made: [1]

Assumption 1. *The extent of the parametric uncertainties and uncertain nonlinearities is known, i.e.,*

$$\begin{array}{l} \theta \in \Omega_\theta \Rightarrow \{\theta : \ \theta_{min} \leq \theta \leq \theta_{max}\} \\ \widetilde{\Delta} \in \Omega_\Delta \Rightarrow \left\{\widetilde{\Delta} : \ ||\widetilde{\Delta}|| \leq \delta_\Delta\right\} \end{array} \tag{14}$$

where $\theta_{min} = [\theta_{1min}, ..., \theta_{(8+2m+2n)min}]^T$, *and* $\theta_{max} = [\theta_{1max}, ..., \theta_{(8+2m+2n)max}]^T$ *are known.* δ_Δ *is a known function.*

The control objective is to synthesize a control input $\mathbf{u_t}$ such that $\mathbf{q} = [x, y]^T$ tracks the reference trajectory $\mathbf{q_d}(t) = [x_d, y_d]^T$ describing the desired contour as closely as possible. $\mathbf{q_d}(t)$ is assumed to be of at-least second-order differentiable.

[1] For simplicity, the following notations are used: $\bullet_i$ for the i-th component of the vector $\bullet$, $\bullet_{min}$ for the minimum value of $\bullet$, and $\bullet_{max}$ for the maximum value of $\bullet$. The operation $\leq$ for two vectors is performed in terms of the corresponding elements of the vectors.

3 Discontinuous Projection

Let $\widehat{\theta}$ denote the estimate of θ and $\widetilde{\theta}$ the estimation error (i.e., $\widetilde{\theta} = \widehat{\theta} - \theta$). In view of (14), the following adaptation law with discontinuous projection modification can be used

$$\dot{\widehat{\theta}} = Proj_{\widehat{\theta}}(\Gamma\tau) \tag{15}$$

where $\Gamma > 0$ is a diagonal matrix, τ is an adaptation function to be synthesized later. The projection mapping $Proj_{\widehat{\theta}}(\bullet) = [Proj_{\widehat{\theta}_1}(\bullet_1), ..., Proj_{\widehat{\theta}_p}(\bullet_p)]^T$ is defined in [13] as

$$Proj_{\widehat{\theta}_i}(\bullet_i) = \begin{cases} 0 \; if \; \widehat{\theta}_i = \theta_{imax} \; and \; \bullet_i > 0 \\ 0 \; if \; \widehat{\theta}_i = \theta_{imin} \; and \; \bullet_i < 0 \\ \bullet_i \; otherwise \end{cases} \tag{16}$$

It is shown that for any adaptation function τ, the projection mapping used in (16) guarantees [13]

$$\begin{array}{ll} (P4) & \widehat{\theta} \in \Omega_\theta \Rightarrow \left\{ \widehat{\theta} : \theta_{imin} \leq \widehat{\theta} \leq \theta_{imax} \right\} \\ (P5) & \widetilde{\theta}^T(\Gamma^{-1} Proj_{\widehat{\theta}}(\Gamma\tau) - \tau) \leq 0, \; \forall \tau \end{array} \tag{17}$$

4 Adaptive Robust Control (ARC) Law Synthesis

Define a switching-function-like quantity as

$$\mathbf{s} = \dot{\varepsilon} + \Lambda\varepsilon \tag{18}$$

where $\Lambda > 0$ is a diagonal matrix. Define a positive semi-definite (p.s.d.) function

$$V(t) = \tfrac{1}{2}\mathbf{s^T M_t s} \tag{19}$$

Differentiating V yields

$$\begin{aligned} \dot{V} = \mathbf{s^T}[&\mathbf{u_t} + \mathbf{d_t} + \widetilde{\Delta} - \mathbf{M_q}\ddot{\mathbf{q}}_\mathbf{d} - \mathbf{B_q}\dot{\mathbf{q}}_\mathbf{d} - \mathbf{A_{fq}}\mathbf{S_f}(\dot{\mathbf{q}}) \\ &- \mathbf{F_{rq}}(\mathbf{q}) - \mathbf{B_t}\dot{\varepsilon} - \mathbf{C_t}\dot{\varepsilon} - \mathbf{D_t}\varepsilon + \mathbf{C_t}\Lambda\varepsilon + \mathbf{M_t}\Lambda\dot{\varepsilon}] \end{aligned} \tag{20}$$

where (P2) is used to eliminate the term $\frac{1}{2}\mathbf{s^T}\dot{\mathbf{M}}_\mathbf{t}\mathbf{s}$. Furthermore, viewing (P3), we can linearly parameterize the terms in (20) as

$$\begin{aligned} &\mathbf{M_q}\ddot{\mathbf{q}}_\mathbf{d} + \mathbf{B_q}\dot{\mathbf{q}}_\mathbf{d} + \mathbf{A_{fq}}\mathbf{S_f}(\dot{\mathbf{q}}) + \mathbf{F_{rq}}(\mathbf{q}) + \mathbf{B_t}\dot{\varepsilon} + \mathbf{C_t}\dot{\varepsilon} \\ &+ \mathbf{D_t}\varepsilon - \mathbf{C_t}\Lambda\varepsilon - \mathbf{M_t}\Lambda\dot{\varepsilon} - \mathbf{d_t} = -\Psi(\mathbf{q}, \dot{\mathbf{q}}, t)\theta \end{aligned} \tag{21}$$

where Ψ is a $2 \times (8 + 2m + 2n)$ matrix of known functions, known as the regressor. Thus (20) can be rewritten as

$$\dot{V} = \mathbf{s^T}[\mathbf{u_t} + \Psi(\mathbf{q}, \dot{\mathbf{q}}, t)\theta + \widetilde{\Delta}] \tag{22}$$

Noting the structure of (22), the following ARC law is proposed:

$$\mathbf{u_t} = \mathbf{u_a} + \mathbf{u_s}; \; \mathbf{u_a} = -\Psi(\mathbf{q}, \dot{\mathbf{q}}, t)\widehat{\theta}; \; \tau = \Psi^\mathbf{T}(\mathbf{q}, \dot{\mathbf{q}}, t)\mathbf{s} \tag{23}$$

where $\mathbf{u_a}$ is the adjustable model compensation needed for achieving perfect tracking and $\mathbf{u_s}$ is a robust control law to be synthesized later. Substituting (23) into (22) and simplifying the resulting expression lead to

$$\dot{V} = \mathbf{s^T}[\mathbf{u_s} - \Psi(\mathbf{q}, \dot{\mathbf{q}}, t)\widetilde{\theta} + \widetilde{\Delta}] \tag{24}$$

The robust control function $\mathbf{u_s}$ consists of two terms:

$$\mathbf{u_s} = \mathbf{u_{s1}} + \mathbf{u_{s2}}, \; \mathbf{u_{s1}} = -\mathbf{K}\mathbf{s} \tag{25}$$

where $\mathbf{u_{s1}}$ is used to stabilize the nominal system, which is chosen to be a simple proportional feedback with $\mathbf{K}$ being a symmetric positive definite matrix for simplicity. And $\mathbf{u_{s2}}$ is a feedback used to attenuate the effect of model uncertainties for a guaranteed robust performance. Noting Assumption 1 and (P4) of (17), there exists a $\mathbf{u_{s2}}$ such that the following two conditions are satisfied

$$\begin{array}{ll} i & \mathbf{s^T}[\mathbf{u_{s2}} - \Psi(\mathbf{q}, \dot{\mathbf{q}}, t)\widetilde{\theta} + \widetilde{\Delta}] \leq \eta \\ ii & \mathbf{s^T u_{s2}} \leq \mathbf{0} \end{array} \tag{26}$$

where η is a design parameter that can be arbitrarily small. One smooth example of $\mathbf{u_{s2}}$ satisfying (24) is given by $\mathbf{u_{s2}} = -\frac{1}{4\eta}h^2\mathbf{s}$, where h is a smooth function satisfying $h \geq ||\theta_\mathbf{M}||||\Psi(\mathbf{q}, \dot{\mathbf{q}}, t)|| + \delta_\Delta$, and $\theta_\mathbf{M} = \theta_{max} - \theta_{min}$.

5 Desired Compensation ARC (DCARC)

In [11], the desired compensation ARC law in which the regressor is calculated by desired trajectory information only to reduce the effect of measurement noise, has been proposed. In the following, a DCARC law employing the cogging force model in (6) is constructed and applied to the biaxial linear-motor-driven gantry as well.

The proposed DCARC law and adaptation function have the same form as (23), but with the regressor $\Psi(\mathbf{q}, \dot{\mathbf{q}}, t)$ substituted by the desired regressor $\Psi_\mathbf{d}(\mathbf{q_d}(t), \dot{\mathbf{q}}_\mathbf{d}(t), t)$:

$$\mathbf{u_t} = \mathbf{u_a} + \mathbf{u_s}; \; \mathbf{u_a} = -\Psi_\mathbf{d}\widehat{\theta}; \; \tau = \Psi_\mathbf{d}^\mathbf{T}\mathbf{s} \tag{27}$$

Choose a positive semi-definite (p.s.d) function:

$$V(t) = \tfrac{1}{2}\mathbf{s^T M_t s} + \tfrac{1}{2}\varepsilon^\mathbf{T}\mathbf{K}_\varepsilon\varepsilon \tag{28}$$

where $\mathbf{K}_\varepsilon$ is a diagonal positive definite matrix. Differentiating $V(t)$ and substituting (27) into the resulting expression yields

$$\dot{V} = \mathbf{s}^{\mathbf{T}}[\mathbf{u_s} + \widetilde{\Psi}\theta - \Psi_{\mathbf{d}}\widetilde{\theta} + \widetilde{\Delta}] + \varepsilon^{\mathbf{T}}\mathbf{K}_\varepsilon\dot{\varepsilon} \tag{29}$$

where $\widetilde{\Psi} = \Psi(\mathbf{q},\dot{\mathbf{q}},t) - \Psi_{\mathbf{d}}(\mathbf{q_d},\dot{\mathbf{q}}_{\mathbf{d}},t)$ is the difference between the actual regression matrix and the desired regression matrix formulations. As shown in [14], $\widetilde{\Psi}$ can be quantified as

$$||\widetilde{\Psi}\theta|| \leq \zeta_1||\varepsilon|| + \zeta_2||\varepsilon||^2 + \zeta_3||\mathbf{s}|| + \zeta_4||\mathbf{s}||||\varepsilon|| \tag{30}$$

where $\zeta_1, \zeta_2, \zeta_3$ and ζ_4 are positive bounding constants that depend on the desired contour and the physical properties of the biaxial gantry. Similar to (25), the robust control function $\mathbf{u_s}$ consists of two terms given by:

$$\mathbf{u_s} = \mathbf{u_{s1}} + \mathbf{u_{s2}},\ \mathbf{u_{s1}} = -\mathbf{K}\mathbf{s} - \mathbf{K}_\varepsilon\varepsilon - \mathbf{K_a}||\varepsilon||^2\mathbf{s} \tag{31}$$

where the controller parameters $\mathbf{K}$, $\mathbf{K}_\varepsilon$ and $\mathbf{K_a}$ are s.p.d. matrices satisfying $\sigma_{min}(\mathbf{K_a}) \geq \zeta_2 + \zeta_4$ ($\sigma_{min}(\cdot)$ denotes the minimum eigenvalue of a matrix) and the following condition

$$\mathbf{Q} = \begin{bmatrix} \sigma_{min}(\mathbf{K}_\varepsilon\Lambda) - \frac{1}{4}\zeta_2 & -\frac{1}{2}\zeta_1 \\ -\frac{1}{2}\zeta_1 & \sigma_{min}(\mathbf{K}) - \zeta_3 - \frac{1}{4}\zeta_4 \end{bmatrix} > 0 \tag{32}$$

Specifically, it is easy to check that if

$$\sigma_{min}(\mathbf{K}_\varepsilon\Lambda) \geq \tfrac{1}{2}\zeta_1 + \tfrac{1}{4}\zeta_2,\ \ \sigma_{min}(\mathbf{K}) \geq \tfrac{1}{2}\zeta_1 + \zeta_3 + \tfrac{1}{4}\zeta_4 \tag{33}$$

the matrix $\mathbf{Q}$ defined in (32) is positive definite. The robust control term $\mathbf{u_{s2}}$ is required to satisfy the following constrains similar to (26),

$$\begin{array}{ll} i & \mathbf{s}^{\mathbf{T}}\left\{\mathbf{u_{s2}} - \Psi_{\mathbf{d}}\widetilde{\theta} + \widetilde{\Delta}\right\} \leq \eta \\ ii & \mathbf{s}^{\mathbf{T}}\mathbf{u_{s2}} \leq \mathbf{0} \end{array} \tag{34}$$

One smooth example of $\mathbf{u_{s2}}$ satisfying (34) is $\mathbf{u_{s2}} = -\frac{1}{4\eta}h_d^2\mathbf{s}$, where h_d is any function satisfying $h_d \geq ||\theta_{\mathbf{M}}||||\Psi_{\mathbf{d}}|| + \delta_\triangle$.

Theorem 1. *[15] The desired compensation ARC law (27) guarantees that:*

A. In general, all signals are bounded. Furthermore, the positive semi-definite function $V(t)$ defined by (28) is bounded above by

$$V(t) \leq exp(-\lambda t)V(0) + \frac{\eta}{\lambda}\left[1 - exp(-\lambda t)\right] \tag{35}$$

where $\lambda = \frac{2\sigma_{min}(\mathbf{Q})}{max[\mu_2, \sigma_{max}(\mathbf{K}_\varepsilon)]}$, and $\sigma_{max}(\cdot)$ denotes the minimum eigenvalue of a matrix.

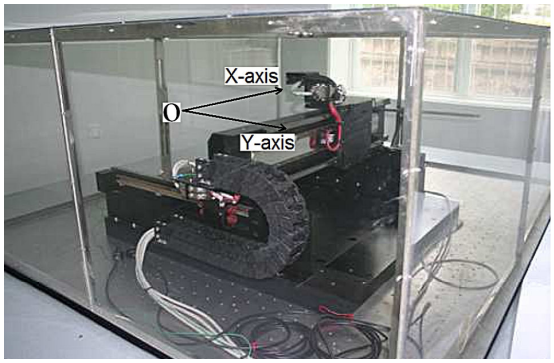

Figure 2. A Biaxial linear motor driven gantry system

B. Suppose that after a finite time t_0 there exist parametric uncertainties only, i.e., $\widetilde{\Delta} = 0$, $\forall t \geq t_0$. Then, in addition to result A, zero final tracking error is also achieved, i.e, $\varepsilon \to 0$ and $\mathbf{s} \to 0$ as $t \to \infty$.

6 Experimental Setup and Results

6.1 Experiment setup

A biaxial Anorad HERC-510-510-AA1-B-CC2 gantry from Rockwell Automation is set up in Zhejiang University as a testbed. As shown in Figure 2, the two axes powered by Anorad LC-50-200 iron core linear motors are mounted orthogonally with X-axis on top of Y-axis. The position sensors of the gantry are two linear encoders with a resolution of $0.5\mu m$ after quadrature. The velocity signal is obtained by the difference of two consecutive position measurements. Standard least-square identification is performed to obtain the parameters of the biaxial gantry and it is found that nominal values of the gantry system parameters without loads are $M_1 = 0.12(V/m/s^2), M_2 = 0.64(V/m/s^2), B_1 = 0.166(V/m/s), B_2 = 0.24(V/m/s), A_{f1} = 0.1(V), A_{f2} = 0.36(V)$.

Explicit measurement of cogging force is then conducted for both axes by blocking the motor and using an external force sensor (HBM U10M Force Transducer with AE101 Amplifier) to measure the blocking forces at zero input voltages. This measurement is done for various positions with 1mm incremental distance. Frequency domain analysis of the measured ripple forces [3] indicates that the fundamental period corresponds to the pitch of the magnets ($P = 50mm$) and that the harmonic terms of cogging forces have significant values at frequencies corresponding to $i = 1,2,3$ and $j = 1,6,12$ in (6). Thus the approximate cogging forces model (6) is chosen as

$$\begin{array}{l} \bar{\mathbf{F}}_{\mathbf{r}}(\mathbf{q}) = [S_{x1}sin(\frac{2\pi}{P}x) + C_{x1}cos(\frac{2\pi}{P}x) + S_{x2}sin(\frac{4\pi}{P}x) \\ \quad + C_{x2}cos(\frac{4\pi}{P}x) + S_{x3}sin(\frac{6\pi}{P}x) + C_{x3}cos(\frac{6\pi}{P}x), \\ \quad S_{y1}sin(\frac{2\pi}{P}y) + C_{y1}cos(\frac{2\pi}{P}y) + S_{y6}sin(\frac{12\pi}{P}y) \\ \quad + C_{y6}cos(\frac{12\pi}{P}y) + S_{y12}sin(\frac{24\pi}{P}y) + C_{y12}cos(\frac{24\pi}{P}y)]^T \end{array} \tag{36}$$

The bounds of the parametric variations are chosen as:

$$\begin{aligned}\theta_{min} &= [0.06, 0.5, 0.15, 0.1, 0.05, 0.08, -0.2, -0.2, -0.2, \\ &\quad -0.2, -0.2, -0.2, -0.2, -0.2, -0.2, -0.2, -0.2, -0.2, \\ &\quad -0.2, -0.5, -1]^T \\ \theta_{max} &= [0.20, 0.75, 0.35, 0.3, 0.15, 0.5, 0.2, 0.2, 0.2, 0.2, \\ &\quad 0.2, 0.2, 0.2, 0.2, 0.2, 0.2, 0.2, 0.2, 0.5, 1]^T\end{aligned} \tag{37}$$

6.2 Performance Indexes

The following performance indexes will be used to measure the quality of each control algorithm:

$\diamond$ $||\varepsilon_c||_{rms} = (\frac{1}{T}\int_0^T |\varepsilon_c|^2 dt)^{1/2}$, the root-mean-square (RMS) value of the contouring error, is used to measure average contouring performance, where T is the total running time;

$\diamond$ $\varepsilon_{cM} = \max_t\{|\varepsilon_c|\}$, the maximum absolute value of the contouring error is used to measure transient performance;

$\diamond$ $||u_i||_{rms} = (\frac{1}{T}\int_0^T |u_i|^2 dt)^{1/2}$, the average control input of each axis, is used to evaluate the amount of control effort.

6.3 Experimental Results

The control algorithms are implemented using a dSPACE DS1103 controller board. The controller executes programs at a sampling period of $T_s = 0.2ms$, resulting in a velocity measurement resolution of $0.0025m/sec$. The following control algorithms are compared:

C1: DCARC without cogging force compensation. The smooth functions $S_f(\dot{x}_d)$ and $S_f(\dot{y}_d)$ are chosen as $\frac{2}{\pi}arctan(9000\dot{x}_d)$ and $\frac{2}{\pi}arctan(9000\dot{y}_d)$. The design parameter Λ is chosen as: $\Lambda = diag[100, 30]$. $\mathbf{u_{s2}}$ in (31) is given in Section V. Theoretically, we should use the form of $\mathbf{u_{s2}} = -\mathbf{K_{s2}}(\mathbf{q})\mathbf{s}$ with $\mathbf{K_{s2}}(\mathbf{q})$ being a nonlinear proportional feedback gain as given in [16] to satisfy the robust performance requirement (34) globally. In implementation, a large enough constant feedback gain $\mathbf{K_{s2}}$ is used instead to simplify the resulting control law. With such a simplification, though the robust performance condition (34) may not be guaranteed globally, the condition can still be satisfied in a large enough working range which might be acceptable to practical applications as done in [17]. With this simplification, noting (31), we choose $\mathbf{u_s} = -\mathbf{K_s}\mathbf{s} - \mathbf{K}_\varepsilon\varepsilon - \mathbf{K_a}||\varepsilon||^2\mathbf{s}$ in the experiments where $\mathbf{K_s}$ represents the combined gain of $\mathbf{K}$ and $\mathbf{K_{s2}}$, and the controller parameters are $\mathbf{K_s} = diag[100, 60]$, $\mathbf{K_a} = diag[10000, 10000]$, and $\mathbf{K}_\varepsilon = diag[5000, 5000]$. The adaptation rates are set as $\Gamma = diag[10, 10, 10, 10, 1, 1, 0, 0, 0, 0, 0, 0, 0, 0, 0, 0, 0, 0, 5000, 5000]$. The initial parameter estimates are chosen as: $\widehat{\theta}(0) = [0.1, 0.55, 0.20, 0.22, 0.1, 0.15, 0, 0, 0, 0, 0, 0, 0, 0, 0, 0, 0, 0, 0, 0]^T$.

C2: DCARC with cogging force compensation. The same control law as the above DCARC but with cogging force compensation, i.e., letting $\Gamma = diag[10, 10, 10, 10, 1, 1, 500, 500, 500, 500, 500, 500, 500, 500, 500, 500, 500, 500, 5000, 5000]$.

The following test sets are performed:

Table 1. Circular contouring results

	Set 1		Set 2		Set 3	
Controller	C1	C2	C1	C2	C1	C2
$\|\|\varepsilon_c\|\|_{rms}(\mu m)$	2.54	1.64	2.66	1.74	3.03	2.11
$\varepsilon_{cM}(\mu m)$	9.22	7.05	9.56	7.91	28.48	25.26
$\|\|u_x\|\|_{rms}(V)$	0.26	0.26	0.26	0.26	0.26	0.26
$\|\|u_y\|\|_{rms}(V)$	0.41	0.41	0.42	0.42	0.41	0.41

Set1 : To test the nominal contouring performance of the controllers, experiments are run without payload;

Set2 : To test the performance robustness of the algorithms to parameter variations, a 5 kg payload is mounted on the gantry;

Set3 : A large step disturbance (a simulated 0.6 V electrical signal) is added to the input of Y axis at t=1.9 sec and removed at t=4.9 sec to test the performance robustness of each controller to disturbance.

6.3.1 Circular contouring with constant velocity

The biaxial gantry is first commanded to track a circle given by

$$\mathbf{q_d} = \begin{bmatrix} x_d(t) \\ y_d(t) \end{bmatrix} = \begin{bmatrix} 0.15sin(2t) \\ -0.15cos(2t) + 0.15 \end{bmatrix} \tag{38}$$

which has a desired velocity of $v = 0.3m/sec$ on the contour.

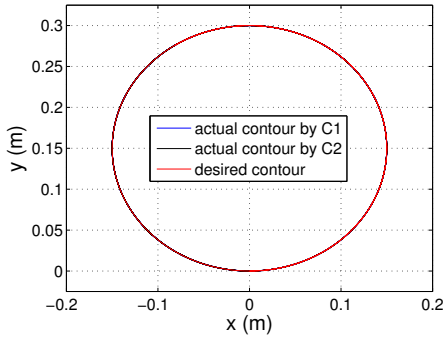

Figure 3. Circular contouring of Set1 in XY plane

The circular contouring experimental results in terms of performance indexes after running the gantry for one period are given in Table 1. Overall, both C1 and C2 achieve good steady-state contouring performance during fast circular movements. As seen from the table, C2 performs much better than C1 in terms of all the indexes with using almost the same amount of control efforts for every test set. For Set1, the desired circle and the actual

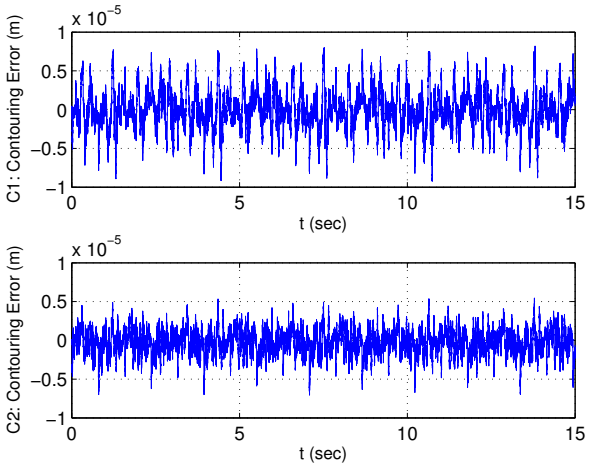

Figure 4. Circular contouring errors of Set1 (no load)

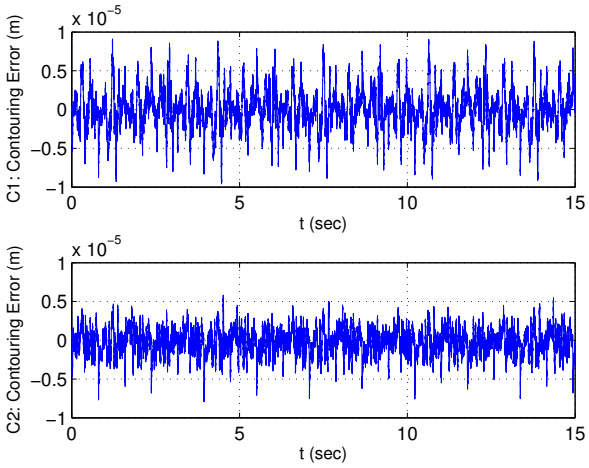

Figure 5. Circular contouring errors of Set2 (loaded)

contours by C1 and C2 are shown in Figure 3, and the contouring errors are given in Figure 4, demonstrating the good nominal performance of DCARC controllers – the contour errors are mostly within 5 μm. For Set2, the contouring errors are displayed in Figure 5 which shows that both controllers achieve good steady-state contouring performance in spite of the change of inertia load, verifying the performance robustness of the proposed DCARC controllers to parameter variations. The contouring errors of Set3 are given in Figure 6. As seen from the figures, the added large disturbances do not affect the contouring performance much except the transient spikes when the sudden changes of the disturbances occur – even the transient tracking errors are within 26 μm for C2. These results demonstrate the strong performance robustness of the DCARC schemes. Comparing C2 with C1, the improvements of contouring performances in all three sets also illustrate the effectiveness of the cogging force compensations.

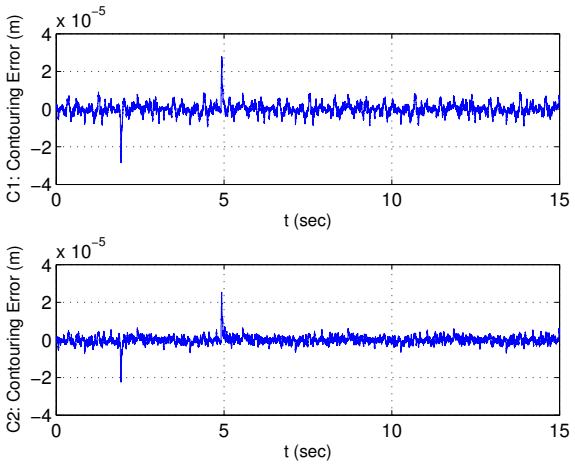

Figure 6. Circular contouring errors of Set3 (disturbances)

6.3.2 Elliptical contouring with constant angular velocity The biaxial gantry is also commanded to track an ellipse described by

$$\mathbf{q_d} = \begin{bmatrix} x_d(t) \\ y_d(t) \end{bmatrix} = \begin{bmatrix} 0.2sin(3t) \\ -0.1cos(3t) + 0.1 \end{bmatrix} \tag{39}$$

which has an angular velocity of $\omega = 3rad/sec$. The elliptical contouring experimental results in terms of performance indexes after running the gantry for one period are given in Table 2. Overall, both C1 and C2 achieve good steady-state contouring performance during the fast elliptical movements. As seen from the table, C2 performs better than C1 in terms of all the indexes with using almost the same amount of control efforts for every test set. For Set1, the desired ellipse and the actual contours by C1 and C2 are shown in Figure 6.3.2. All these results further demonstrate the strong performance robustness of the proposed

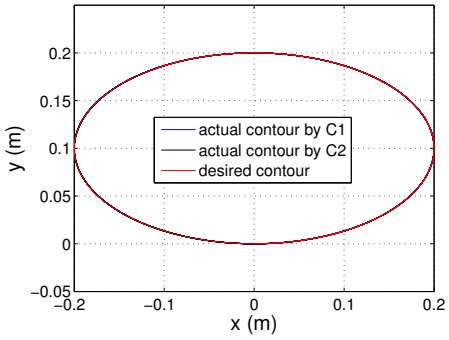

Figure 7. Elliptical contouring of Set1 in XY plane

	Set 1		Set 2		Set 3	
Controller	C1	C2	C1	C2	C1	C2
$\|\|\varepsilon_c\|\|_{rms}(\mu m)$	2.66	2.06	2.74	2.10	3.43	2.93
$\varepsilon_{cM}(\mu m)$	8.77	7.33	9.69	8.55	31.03	29.46
$\|\|u_x\|\|_{rms}(V)$	0.35	0.35	0.37	0.37	0.35	0.35
$\|\|u_y\|\|_{rms}(V)$	0.50	0.50	0.52	0.51	0.50	0.50

Table 2. Elliptical contouring results

schemes and the effectiveness of the cogging force compensations.

7 Conclusions

This paper studies the high-performance contouring motion control of an industrial biaxial linear-motor-driven precision gantry subject to significant nonlinear cogging force effects. A desired compensation ARC controller has been developed under the task coordinate formulation. The proposed controller explicitly takes into account the effect of model uncertainties coming from the inertia load, friction forces, cogging forces and external disturbances. In particular, based on the special structure of the cogging forces, design models consisting of known basis functions with unknown weights are used to approximate the unknown nonlinear cogging forces in both axes. The resulting controller guarantees a prescribed contouring performance in general while achieving asymptotic tracking in the presence of parametric uncertainties only. Experimental results for both high-speed circular and elliptical motions have demonstrated the excellent contouring performance of the DCARC scheme and the effectiveness of the proposed cogging force compensations in actual applications.

REFERENCES

[1] Cheng, M.-Y., and Lee, C.-C., 2007. "Motion controller design for contour-following tasks based on real-time contour error estimation". *IEEE Transactions on Industrial Electronics,* **54**(3), June, pp. 1686–1695.

[2] Koren, Y., and Lo, C. C., 1992. "Advanced controllers for feed drives". *CIRP Proc.-Manufacturing Systems,* **41**(2), pp. 689–698.

[3] Lu, L., Chen, Z., Yao, B., and Wang, Q., 2008. "Desired compensation adaptive robust control of a linear motor driven precision industrial gantry with improved cogging force compensation". *IEEE/ASME Transactions on Mechatronics,* **13**(6), December, pp. 617–624.

[4] Koren, Y., 1980. "Cross-coupled biaxial computer control for manufacturing systems". *ASME J. Dynamical Systems, Measurement, and Control,* **102**, pp. 265–272.

[5] Yeh, S.-S., and Hsu, P.-L., 2002. "Estimation of the contouring error vector for the cross-coupled control design". *IEEE/ASME Transactions on Mechatronics,* **7**(1), March.

[6] Su, K.-H., and Cheng, M.-Y., 2008. "Contouring accuracy improvement using cross-coupled control and position error compensator". *International Journal of Machine Tools and Manufacture,* **48**, pp. 1444–1453.

[7] Chiu, G. T.-C., and Tomizuka, M., 2001. "Contouring control of machine tool feed drive systems: a task coordinate frame approach". *IEEE Trans. Control System Technology,* **9**, Jan., pp. 130–139.

[8] Chen, C.-L., and Lin, K.-C., 2008. "Observer-based contouring controller design of a biaxial stage system subject to friction". *IEEE Transactions on Control System Technology,* **16**(2), March, pp. 322–329.

[9] Otten, G., Vries, T., Amerongen, J., Rankers, A., and Gaal, E., 1997. "Linear motor motion control using a learning feedforward controller". *IEEE/ASME Transactions on Mechatronics,* **2**(3), pp. 179–187.

[10] Yao, B., Hu, C., and Wang, Q., 2007. "Adaptive robust precision motion control of high-speed linear motors with online cogging force compensations". In IEEE/ASME Conference on Advanced Intelligent Mechatronics, pp. 1–6.

[11] Yao, B., 1998. "Desired compensation adaptive robust control". In The ASME IMECE, Vol. 64, pp. 569–575.

[12] Braembussche, P. V., Swevers, J., Brussel, H. V., and Vanherck, P., 1996. "Accurate tracking control of linear synchronous motor machine tool axes". *Mechatronics,* **6**(5), pp. 507–521.

[13] Yao, B., 1997. "High performance adaptive robust control of nonlinear systems: a general framework and new schemes". In IEEE Conf. on Decision and Control, pp. 2489–2494.

[14] Sadegh, N., and Horowitz, R., 1990. "Stability and robustness analysis of a class of adaptive controllers for robot manipulators". *Int. J. Rob. Res.,* **9**(3), pp. 74–92.

[15] Hu, C., Yao, B., and Wang, Q., 2009. "Coordinated adaptive robust contouring control of an industrial biaxial precision gantry with cogging force compensations". *IEEE Transactions on Industrial Electronics* (revision is under review).

[16] Yao, B., and Tomizuka, M., 1997. "Adaptive robust control of siso nonlinear systems in a semi-strict feedback form". *Automatica,* **33**(5), pp. 893–900.

[17] Yao, B., Bu, F., Reedy, J., and Chiu, G. T.-C., 2000. "Adaptive robust control of single-rod hydraulic actuators: theory and experiments". *IEEE/ASME Transactions on Mechatronics,* **5**(1), pp. 79–91.